Retrofitting Southern African cities: a call for appropriate rooftop greenhouse designs as climate adaptation strategy

Jan Hugo[a,*], Chrisna du Plessis[a] and Andries Masenge[b]

[a]Department of Architecture, University of Pretoria, Corner of Lynwood and Roper Street, Hatfield, Pretoria, South Africa

[b]Department of Statistics, University of Pretoria, Corner of Lynwood and Roper Street, Hatfield, Pretoria, South Africa

*Corresponding author. jan.hugo@up.ac.za

Highlights

- Passively controlled non-integrated rooftop greenhouses adversely affect the associated building's indoor temperatures .
- Thermal impacts are exacerbated by climate change affected climatic conditions.
- Ensure rooftop greenhouses are context-specific and bioclimatic appropriate designs to realise co-benefits.

Abstract

In response to the burgeoning building integrated agriculture (BIA) discourse and industry, and assumptions of this land use form as a climate change adaptation strategy, this study considers the impact of rooftop greenhouses (RTGs) on the thermal performance of the built environment in current and future climate conditions. Based on empirical evidence, the study simulates the thermal impact of completely retrofitting an existing building in a Southern African urban context with passively controlled, non-integrated RTGs under current and future climate change affected climatic conditions. The study concludes that the current greenhouse technologies used in South African rooftop farms provide limited thermal modulation capacity for farmers, as well as generally negatively affecting the thermal performance of the associated buildings. Simulating both highly and poorly insulated buildings reveal contrasting impacts on the indoor thermal environment, with a 0.73°C decrease and 0.55°C increase in mean temperatures, respectively. Conversely, the highly insulated simulation reveals an annual energy consumption increase of 3.5%, which progressively worsens under higher climate change induced temperatures. These findings, based on current practices in the BIA industry, hope to inform both the choice of technology,

as well as the development of appropriate greenhouse technologies to maximise their performance and enable co-benefits as often assumed in the industry.

Keywords: urban agriculture, climate change, thermal performance, building performance modelling, appropriate technologies, building integrated agriculture.

1. Introduction

The current climate crisis that is indiscriminately affecting cities worldwide calls for adjustments to the built environment to both increase its resource efficiency and improve its resilience to the expected climate change hazards. Within cities, several opportunities exist to radically adjust certain land-use practices and rapidly increase their implementation to make consequential changes to adapt to future climatic changes. Urban agriculture (UA) and building integrated agriculture (BIA) offers a range of such opportunities.

Dubbeling and De Zeeuw (2011) identified local food production through UA as a strategy to not only lower the energy inputs, but also enable resource circularity and cascading energy use opportunities in cities. Enabling local food production is, therefore, a viable option for cities to lower the energy inputs of food resources and harness the associated co-benefits of these land-use practices.

To date several studies promote multiple co-benefits that UA and BIA present to the city (Dubbeling and De Zeeuw, 2011; Thomaier et al., 2014). Goldstein et al. (2016) identify several additional in-situ and ex-situ co-benefits that BIA enables, amongst others the reduction of carbon footprints and limiting urban heat island effects. Castleton et al. (2010) and Thomaier et al. (2014) propose that the use of growing systems can improve thermal insulation properties, provide additional shading, and capture residual heat for local use.

However, while several studies promote the co-benefits associated with BIA, there is a dearth of research into the performance of BIA, specifically rooftop greenhouses (RTGs), in temperate subtropical climates and developing contexts. This study investigated the thermal performance of existing passively controlled, non-integrated RTGs implemented in South African conditions, and based on these findings, simulated their potential to modulate the indoor thermal environment in current and future climate change affected conditions in Tshwane, South Africa.

After providing some background to UA and RTG, this article first presents the method used to verify and simulate the thermal impacts of the RTGs and then discusses the field data used to verify the simulations. It then discusses the simulation findings, and their implication

for potential technological adjustments needed to improve the performance of RTGs in similar conditions.

2. Background

Caplow (2009) originally defined BIA as high performance hydroponic systems that use renewable or recovered water and energy resources, effectively changing the local urban metabolism. Specht et al. (2014) provide the broader definition of zero-acreage farming, which includes indoor farms, rooftop gardens and rooftop greenhouses (RTGs), as innovative land-use forms that limit the use of land in cities, improve resource recycling, shorten the production and consumption networks, and improve the local energy efficiency. This study used a more inclusive definition of BIA farms, as argued by Orsini (2020), proposing that all forms of agriculture integrated with the built environment present opportunities for low energy food production, and thermal and efficient energy co-benefits.

Globally there has been a proliferation of BIA projects, specifically the development of RTGs (free-standing greenhouses on rooftops) and I-RTGs (rooftop greenhouses integrated with the services and/or structure of the building). The most prominent projects are typically located in highly successful cities, for example Gotham Greens in New York, Lufa Farms in Montreal, BHIG in Brussels, and ComCrops in Singapore. These novel BIA projects are not only associated with affluent cities, but are also implemented in developing contexts such as Johannesburg, South Africa (Davie, 2018). As a result, this novel land-use form is developing both as discourse and industry.

As a rapidly growing discourse, BIA's close integration with the built environment is promoted by many as effective strategies to promote sustainable urban regeneration. Orsini et al. (2015), argue that rooftop agriculture (BIA farm type) can optimise land-use efficiency, diversify local income streams, increase the multivalence of spaces, and improve resource efficiency through optimised waste streams and water consumption. Due to the implementation flexibility in diverse contexts, using a variety of technologies, and including multiple stakeholders (Nasr et al., 2017),many advocate using different features of the built environment as productive spaces that utilise reciprocal urban regenerative processes (Nelli, 2020).

Integrated rooftop greenhouses (I-RTGs) is one of the BIA land-use forms that has developed significantly as a viable sustainable food production solution as argued by Sanyé-Mengual et al. (2015) . The close integration of the RTGs with the built environment allows for metabolic exchanges between farms and buildings improving their resource efficiency (Sanyé-Mengual et al., 2018). Several studies have considered the performance of the I-RTGs and conclude that they are highly efficient in retaining thermal energy to improve

growing conditions, capture and distribute waste heat, harvest and use rainwater, as well as capture carbon dioxide to stimulate plant growth (Benis et al., 2017; Sanyé-Mengual et al., 2018; Nadal et al., 2017). As a result, the integration of I-RTGs with the built environment presents several resource efficiency co-benefits.

Unfortunately, the interest in the co-benefits of BIA is often based on assumptions with limited empirical research. Only recently have studies started to model and assess their impacts on the built environment. Furthermore, limited research has considered the performance and impacts of RTGs in temperate to hot climates. As a result, several projects are being implemented in cities throughout these warmer regions with little understanding of their performance. Notably, most studies on RTGs and I-RTGs were conducted in colder climates highlighting lower heating loads resulting from retrofitting buildings with RTGs. Studies by Benis et al. (2015) and Sanyé-Mengual et al. (2018), conclude that the I-RTGs affects the built environment differently in hotter climates: in these contexts the additional residual heat require alternative modes of utilisation as limited indoor heating is needed.

In response to this knowledge gap, this study considered passively controlled non-integrated RTG's that are currently implemented in South African cities to simulate and assess their reciprocal impact on the associated buildings.

3. Materials and Methods

Following a pragmatism paradigm, the study critically analysed current RTGs implemented in South Africa and their impact on the built environment. The research process followed three phases. Initially, a data collection phase documented existing RTGs in Johannesburg, South Africa. Secondly a simulation phase verified the model parameters based on these existing RTGs. Finally, simulations were undertaken using the defined model parameters and applying them to a theoretical building located in Tshwane, South Africa. These simulations assessed the thermal impacts of passively controlled non-integrated RTGs on the associated buildings in current and predicted future climatic conditions.

3.1. First phase: Data collection and fieldwork.

To consider the performance of RTGs within the Southern African context, four rooftop urban farms were identified and monitored during the 2019/2020 summer and winter periods. The four rooftop farms are all located in Johannesburg, South Africa. While the surrounding contexts of all four farms differ, they all share similar materials, construction characteristics, growing systems, and crop varieties. Although the sample group is located in an alternative city than the final simulated context, the metropolitan areas of Johannesburg and Tshwane

form an urban conurbation known as the Gauteng city-region. The two cities have negligible climatic differences, and any climatic deviations were accounted for in the simulations.

Upon verifying the general performance trends of the four farms, a single farm was used to verify the model parameters. This farm is located in New Doornfontein, Johannesburg. It is located on the roof of a seven-storey building (25m high and experiences no overshadowing or wind protection.

Similar to the other greenhouses, the farm in New Doornfontein uses an RTG structure with a composite envelope consisting of knitted high-density polyethylene (HDPE) (40% shading) layered on top of white translucent Poly-Ethylene-vinyl acetate (Poly-EVA) sheeting. The envelope is fixed to vaulted galvanised steel sub-frames. The greenhouse does not employ any active climate control measures and uses an NFT hydroponic growing system. The crops grown in the greenhouse consist of various leafy greens and herbs.

The data collection was undertaken during both the summer and winter periods, and each site was documented for at least five consecutive days at a time. At each site the micro-climatic data were collected, including the ambient temperature (T_a), relative humidity (RH) and globe temperature (T_g) (Fig. 1). These were documented at three positions in each site: outside the greenhouse on the open exposed roof referred to as *open location*, and inside the RTG on the northern and southern boundaries. In addition, a portable weather station collected the microclimatic data on the open roof.

Figure 1: Sensors used to document both the internal and external climatic conditions.

The data collection used SSN-22 USB temperature/humidity loggers to collect the ambient temperature and relative humidity conditions both inside and outside the RTG. The SSN-22 USB logger continually logged the conditions and has a ±3% (RH) and ±0.3°C (AT) accuracy. An AZ87786 Portable heat index monitor and data logger with a 75mm black ball

was used to collect the globe temperature conditions. It has a response time of 15 minutes and ±1.5°C (GT) accuracy. Based on the research findings of Liang et al. (2014), the impact of vegetation on the microclimate can be measured within 1m from a surface. These instruments were therefore located at 500mm above the finished floor level, aligned with the first planted tier of the NFT planting system. The instruments were also protected using white reflective shields to limit any impacts from direct overhead solar radiation. An HP2000 Wi-Fi wireless weather station was also used to document the local microclimate on the roof.

The study did not measure the thermal impact in the spaces below the greenhouse structures as i) access was limited, ii) diverse indoor environment conditions (naturally ventilated, completely open, and air-conditioned conditions) were present, iii) the farms never covered the whole roofs. As a result, simulations were used to assess the impact of the RTGs.

3.2. Second phase: Verifying the simulation model.

The second phase used the field data to simulate and verify the modelling parameters. It followed a two phased modelling process similar to a study by Skelhorn et al. (2016). This involved modelling the microclimate, adjusting the local weather file accordingly, and simulating the final model using the adjusted climatic conditions. The simulations were conducted using ENVImet and IESve. ENVImet is effective in modelling the urban environment on a three-dimensional basis, and considers the impact of material choices, vegetation, wind and solar radiation fluxes within the urban context (ENVIMET, 2018). IESve is an ISO 7730 validated analysis tool, which uses the EnergyPlus simulation engine to simulate the performance of a building within specific climatic context (IES, 2018).

During the first simulation phase, the microclimate on the roof of the New Doornfontein site was modelled using ENVImet. The simulated and measured microclimate data achieved a correlation coefficient of 0.79 (Pearson's R). Using the findings from the ENVImet model, the thermal variations between the ground and roof level conditions were compared and changes in microclimatic conditions were used to adjust the weather file to simulate and verify the RTG using IESve.

Many studies have developed dynamic models of greenhouses to optimise the energy consumption of climate controlled greenhouses (Beveren et al., 2015; Graamans et al., 2018; Serir et al., 2012). These studies use MATLAB, KASPRO and TRNSYS to calculate the energy balance within these greenhouse structures. As dynamic models these analyses considered the energy inputs via local climatic conditions and incident radiation, the material performance of the greenhouse to control the indoor environment, and artificial climate control strategies to optimise the growing conditions.

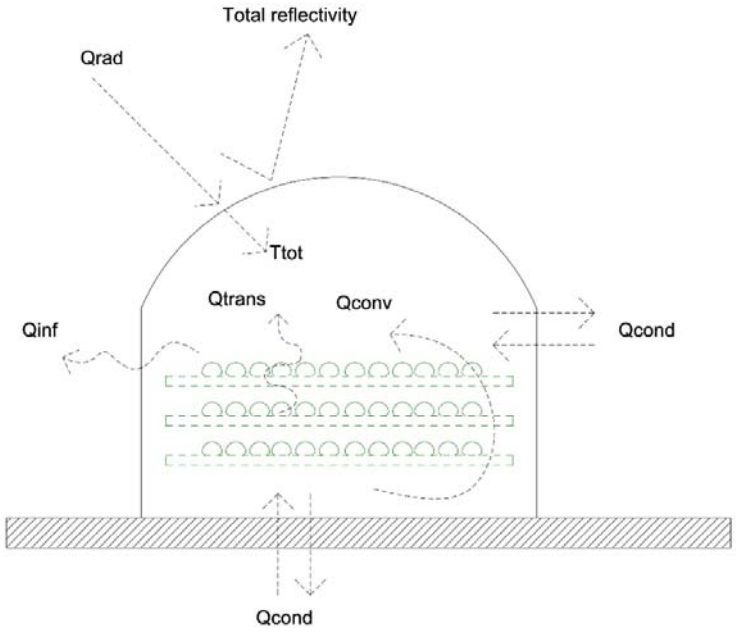

Figure 2: Theoretical thermal energy balance within an RTG

As this study did not set out to control the indoor environment, but rather document the RTG's resultant impact on the associated building structure, the IESve model was developed to replicate the current performance in practice and only modelled the energy inputs as documented on site (Fig 2). The energy balance taking place in the greenhouse is reflected in equation 1.

$$Qrad - (Qinf + Qevap + Qconv + Qcond) = 0 \quad \text{(EQ1)}$$

Equation 1 assumes a basic energy balance, with the total incident radiation (Q_{rad}) representing the total energy added to the greenhouse interior (EQ2). Energy losses take place through infiltration and air leakage (Q_{inf}). The Q_{inf} was observed onsite and adjusted to ensure model verification. The conversion of sensible thermal energy into latent thermal energy is accounted for through the plant evapotranspiration calculation (Q_{evap}) (EQ4). The total energy lost through convection (Q_{conv}) is considered as zero in this study as no artificial or passive ventilation strategies were observed on site. Finally, the energy lost through conduction (Q_{cond}) is accounted for in the IESve model (EQ7).

$$Qrad = Ttot.Irad \quad \text{(EQ2)}$$

Q_{rad} was calculated by multiplying the total incident radiation (I_{rad}), based on the EPW weather file for the given location, with the total composite transmissivity of the greenhouse envelop (T_{tot}) (EQ2; Table2). Both envelope 1 (env1) and envelope 2 (env2) have specific transmissivities and were considered as a composite material in the model (EQ3) (Table 2).

$$Ttot = (Tenv1).(Tenv2) \quad \text{(EQ3)}$$

The latent thermal energy conversion due to the plant evapotranspiration was included using an adjusted Penman-Monteith equation (FAO-PM) developed by Allen et al. (1998). The simplified FAO-PM uses the local latitudinal location, local climatic conditions, and a reference crop to calculate the latent thermal conversion ($Qlat$) (EQ4).

$$Qlat = \frac{\Delta(Rn-G)+\gamma\frac{900}{T+273}u_{2(e_s-e_a)}}{\Delta+\gamma(1+0.34u_2)} \quad \text{(EQ4) (Allen et al., 1998)}$$

The FAO-PM equation (EQ4) allows for adjustable variables such as specific growing conditions and the crop coefficient. Rn accounts for the net radiation at the crop surface. In this study, G represented the heat flux affected by the concrete roof on which the greenhouse is constructed. The mean daily temperature (T), saturated vapour pressure (e_s), actual vapour pressure (e_a), and slope of the vapour pressure curve (Δ) were derived from the local weather file. The wind speed (u_2) within the greenhouse was measured on site, the lack of active and passive cooling strategies resulted in a negligible wind speed of 0.01m.s. The psychrometric constant (y) was derived from the atmospheric pressure and elevation above sea level. While the FAO-PM uses a conversion factor to calculate the evapotranspiration (mm/day) based on the latent thermal flux, the study excluded this factor from the final calculations.

As undertaken in the work of Graamans et al. (2018) the thermal flux due to the latent thermal conversion of the plants inside the greenhouse is included in the model as a negative sensible heat gain. The $Qevap$ was derived as a negative heat source per square meter (W/m^2) and adjusted on an hourly basis according to the general plant coverage coefficient (A_{cov}) (EQ6), monthly mean incident radiation coefficient (I_{rmonth}), and daily available sunlight (Irr_{daily}) (EQ5).

$$Qevap = Qlat.A_{cov}.\frac{Irradiance_{monthly\ mean}}{Irradiance_{maximum\ monthly\ mean}}.\frac{Irradiance_{hourly\ mean}}{Irradiance_{maximum\ mean}} \quad \text{(EQ5)}$$

The general plant coverage coefficient (A_{cov}) was calculated by comparing the growing systems' area coverage with the overall size of the RTGs and using the mean average (EQ6).

$$A_{cov} = Mean\ Area_{growing\ system}/Mean\ Area_{greenhouse}$$

$$A_{cov} = 0.48 \text{ (EQ6)}$$

The energy lost through conduction (Q_{cond}) is affected by the insulating capacity of the greenhouse membranes and the concrete roof as ground plane, and is defined as the

cumulative thermal resistance (u) (Table 2). The total area of the respective surfaces (A), as well as the thermal difference (Δt) between the greenhouse interior and exterior temperature were included in the calculation (EQ7).

$$Qcond = (A_1.u_1.\Delta t_1) + (A_2.u_2.\Delta t_2) \dots (A_x.u_x.\Delta t_x) \quad \text{(EQ7)}$$

The verification phase compared the measured internal and external ambient temperatures with the simulated internal and external ambient temperatures. This involved both a visual assessment of the temperature variations, and replicating the correlation coefficients of the measured temperatures with the simulated thermal conditions. The final measured and simulated correlation coefficients for the Pearson's R analysis are 0.99 and 0.89 respectively, while the standard deviations of the temperature distribution were 2.5°C and 2.48°C respectively. These findings verified the RTG simulation parameters used in the final simulation phase of the theoretical building in Tshwane.

3.3. Third Phase: Simulating the theoretical models.

The final simulation, undertaken in the Tshwane context, simulated the impact of retrofitting the whole roof of a theoretical building with RTGs (Fig. 3). In addition to using the same RTG simulation parameters established in the second phase, the third phase considered the thermal performance of a typical office building. The study modelled a typical five storey office building, the building function was chosen due to the homogeneity in construction and use. An occupancy density of 15m^2 per person and a typical occupancy schedule 8h/day for 5d/week was used (South Africa, 2011).

Basic internal gains of sensible (70W) and latent (55W) thermal loads were assumed for the building occupants (ASHRAE, 2017). The plug load density was assumed at 15W/m^2 and lighting density at 12W/m^2 (South Africa, 2011). A 100% conversion of lighting and equipment energy to sensible thermal energy was assumed.

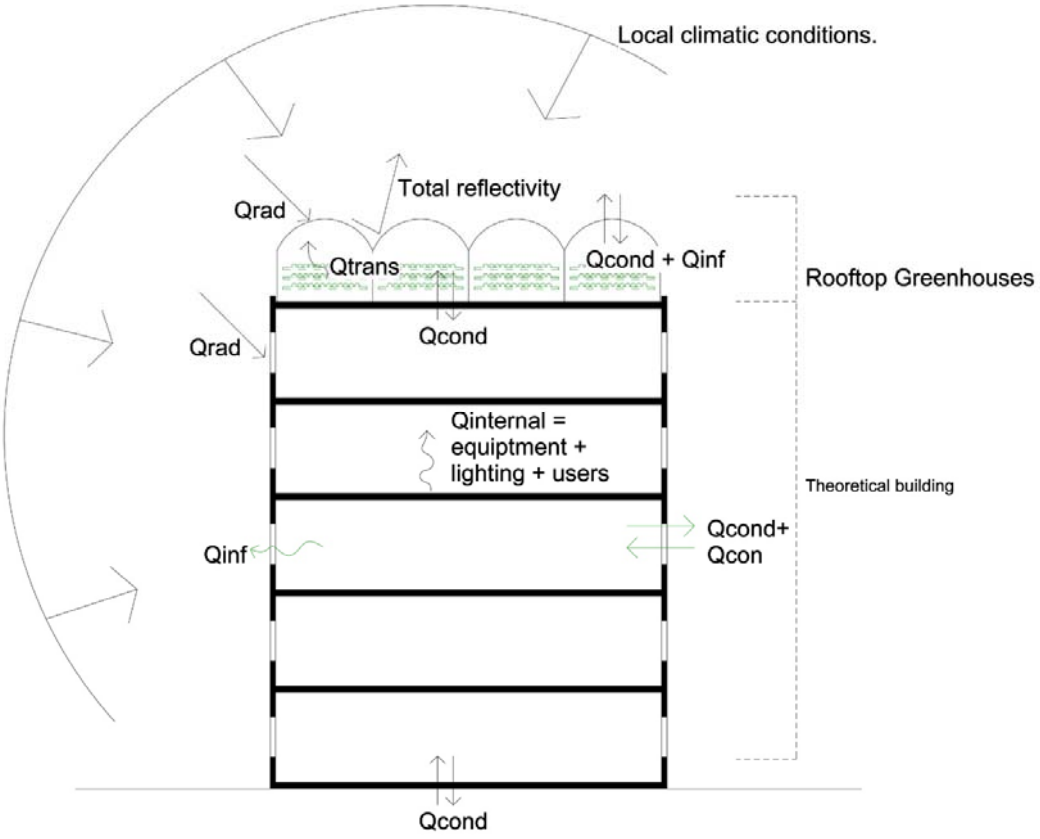

Figure 3: Theoretical model energy flows within the simulated model.

Two models were considered during the simulation, in each case the models were either completely retrofitted with RTGs or not retrofitted at all. The first model incorporated higher insulation standards as per the local South African SANS 10400XA standards promulgated in 2011 (South Africa, 2011), while the second model tested a poorly insulated building as typically found in the Tshwane context. The building construction parameters are discussed in Table 1, with the higher insulated building differing in roof construction (R-value: 3.76 m^2K/W vs 1.19 m^2K/W), adhering to stricter infiltration standards, and using double glazing. Finally, both models used a 30% floor-to-glazed area ratio.

Table 1: Basic construction parameters of simulation models.

	Highly insulated model – SANS 10400 XA compliant	**Poorly insulated model– SANS 10400 XA non-compliant**	**References**
Ground Floor	100mm Concrete slab (No insulation) – R-value = 0.79; U-value = 1.273	100mm Concrete slab (No insulation) – R-value = 0.79; U-value = 1.273	SANS 10400 XA (South Africa, 2011) and assumed conditions.
First Floor (all other floors)	255mm reinforced concrete Slab – R-Value = 0.38; U-value = 2.617	255mm reinforced concrete Slab – R-Value = 0.38; U-value = 2.617	
Walls	230mm masonry wall, plastered on both sides - R-value = 0.48*; U-value = 2.067 SANS 10400 stipulates 230mm masonry walls comply.	230mm masonry wall, plastered on both sides - R-value = 0.48; U-value = 2.067	
Roof	255mm Concrete slab with 120mm expanded polystyrene insulation and waterproofing - total R-value = 3.76; U-value = 0.266	255mm Concrete slab with 30mm expanded polystyrene insulation and waterproofing Total R-value = 1.19; U-value = 0.841	
Glazing (30% glazing ratio)	Aluminium frame, double pane (6mm clear glass) - U-value = 2.88; SHGF = 0.78	Aluminium frame, single pane (6mm clear glass) - U-value = 5.17; SHGF = 0.78	

The simulations that included the retrofitted RTGs, assumed a 100% covering of the roof areas with RTGs - total area 570m^2. The construction parameters in the simulations replicated the existing rooftop farms that were documented (Table 2). The envelope construction and material characteristics were derived from literature reviews, observations on site and discussions with contractors that built the greenhouses. The final absorptivity of the Poly-EV lining was adjusted to accommodate for dust settlement on the membrane using Image-J (Conradie, 2017).

While the study considered the ambient temperature impact of retrofitting RTGs on the building interior, it also set out to consider the energy implications of the adjusted indoor ambient temperatures. To simulate changes in energy consumption, an air-conditioning system was included. Based on the current commercially available air-conditioning systems in South Africa, a basic centralised air-conditioning system with a heating seasonal energy efficiency ratio (SEER) and seasonal coefficient performance (SCOP) of 3.4, and the cooling energy efficiency ratio (EER) and SEER of 2.5 and 2.125 respectively, was defined (DOE, 2019). Cooling and heating set points of 25°C and 19°C were used (South Africa, 2011).

Table 2: Simulation parameters of the RTGs modelled in analysis.

	Rooftop Greenhouse Construction	References
Occupation	108m^2 per person.	On-site observations
Occupation Schedule	5 hours daily.	
Climate control	No artificial cooling or heating. No additional artificial lighting.	On-site observations
Planting system	Hydroponic NFT system. Area: 104 m^2, coverage 0.48.	On-site observations
Transpiration impact	Latent energy – 9.36 Watts/m^2 adjusted to 0.48 coverage. Based on FOA-PM equation. Scheduled to accommodate daily fluctuations and seasonal impacts.	Monteith (1965); Allen et al. (1998); Graamans et al. (2018)
Energy load	Electrical water pumps 1.3 Watts/m^2.	On-site observations
Greenhouse construction - Floor	Floor: 255mm concrete slab with water proofing – U-Value: 2.617. As per simulated model – see table 1.	On-site observations
Composite Envelope	Knitted HDPE monofilament netting (0.2mm): Absorptivity – 0.32; Transmission – 0.6; Reflection – 0.08; White Poly Ethelyne Vinyl Acetate (0.2mm): Absorptivity – 0.22; Transmission – 0.45; Reflection – 0.33. Composite Total R-value – 0.201; Total U-value – 4.98	Nijskens et al. (1984); Berge (2009); Al-Helal and Abdel-ghany (2011); ASHRAE (2017); Engineering Toolbox (2019) and observations on site.
Infiltration	Infiltration adjusted to validate model – 30ACH.	Observed on site and verified during simulations.

Tshwane has a temperate climate with hot summers and dry winters (Koppen-Geiger: Cwa) (StepSA, 2020). The simulation models used weather files for both current climatic conditions and adjusted 2100 climatic conditions simulating A2 business-as-usual emission scenarios (IPCC, 2000). Under these adjusted 2100 conditions average temperature increases of 4°C and higher are expected for the Southern African region (DEA, 2013). The weather files were generated using Meteonorm and is based on the local weather data collected from the Proefplaas weather station, located 3km from the theoretical site.

4. Field data: New Doornfontein farm performance data which informed the simulations.

To simulate the thermal impact that RTGs have on buildings in the Southern African region, the study used collected field data of a functioning rooftop farm, New Doornfontein farm, to develop the simulation model. These findings, derived from field data, were used to inform the simulation model.

Analysis of the summer and winter performance of the New Doornfontein farm revealed slight variations in the ambient temperatures at the three site locations. In the winter period, the northern location ($T_{a\ mean}$=16.90°C; $T_{a\ sd}$=6.76°C) has a slightly higher mean temperature than the southern ($T_{a\ mean}$=15.35°C; $T_{a\ sd}$=5.63°C) or the open locations ($T_{a\ mean}$=14.35°C; $T_{a\ sd}$=3.91°C) (Table 3). Furthermore, while similar mean temperatures were documented, the northern location had a higher deviation in temperatures, which is noteworthy when considering the maximum ambient temperature difference between the northern and open location. The analysis revealed a 12.3°C difference between the maximum temperatures at the northern and open locations (34.00 vs 21.70°C).

The summer data of the temperature variations revealed that the northern ($T_{a\ mean}$=23.36°C; $T_{a\ sd}$=6.48°C) and southern locations ($T_{a\ mean}$=23.77°C; $T_{a\ sd}$=7.34°C) perform similarly, with slightly higher mean ambient temperatures than the open location ($T_{a\ mean}$=21.24°C; $T_{a\ sd}$=5.71) (Table 3). The southern location had minimally higher maximum ambient temperatures. 4.7°C higher than the open location.

Table 3: Descriptive Statistics of the summer and winter thermal data.

	Location	N Obs	Mean	Std Dev	Median	Minimum	Maximum
Winter - Ambient Temperature (°C)	North	361	16.90	6.76	15.00	6.30	34.00
	South	361	15.35	5.63	13.90	5.50	25.30
	Open	362	14.35	3.91	14.30	5.80	21.70
Summer - Ambient Temperature (°C)	North	289	23.36	6.48	21.00	15.70	39.10
	South	289	23.77	7.34	20.70	15.50	39.30
	Open	289	21.24	5.71	19.60	14.30	34.60

The slight thermal variations were confirmed during the ANOVA test performed for both periods. In both the winter and summer periods the T_a variations rejected the null-hypothesis (Winter period: F-value=19.34; df=1082; $T_a p<0.0001$) (Summer period F-value=12.41; df=866; $T_a p<0.0001$). The effect size of the difference in the winter period is considered medium ($T_a r^2$=0.034), while in the summer period the effect size is slightly smaller ($T_a r^2$=0.0279) (Cohen, 1988). In both the summer and winter periods there was a statistical difference between the three locations, albeit small to medium.

The visual analysis of the temperature variations is more revealing. In both the summer and winter periods, the temperature graph highlights that the temperatures of all three locations are closely aligned except during the midday period (11:00-15:00). Figures 4 and 5 reveal

that the temperature variations are most pronounced during the hottest period of the day, and most notable during the winter period.

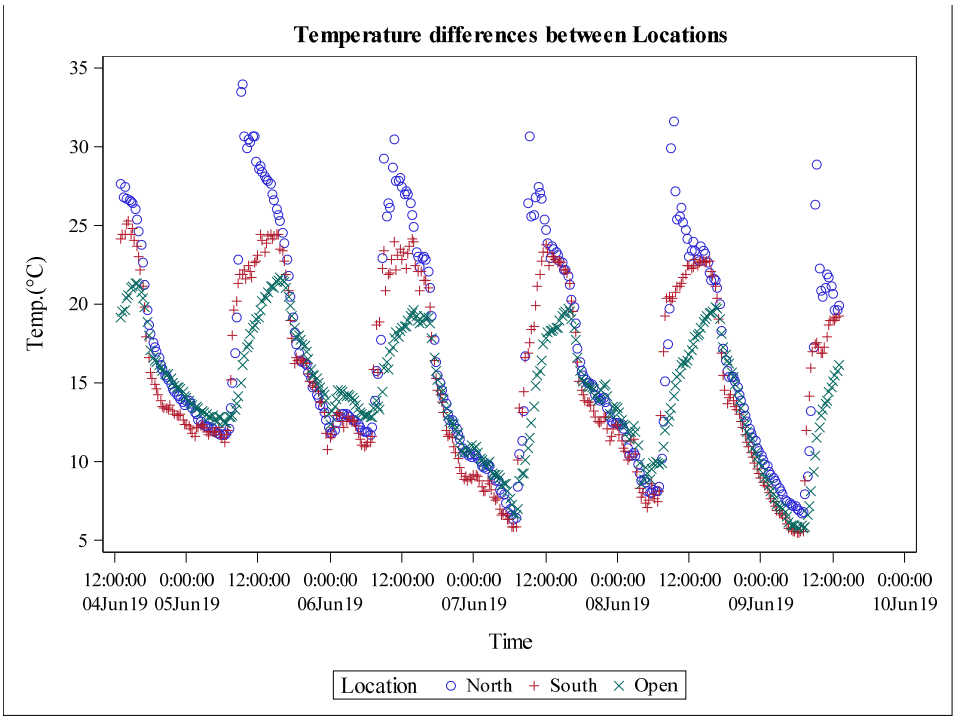

Figure 4: Temperature variations between the three locations - Winter period.

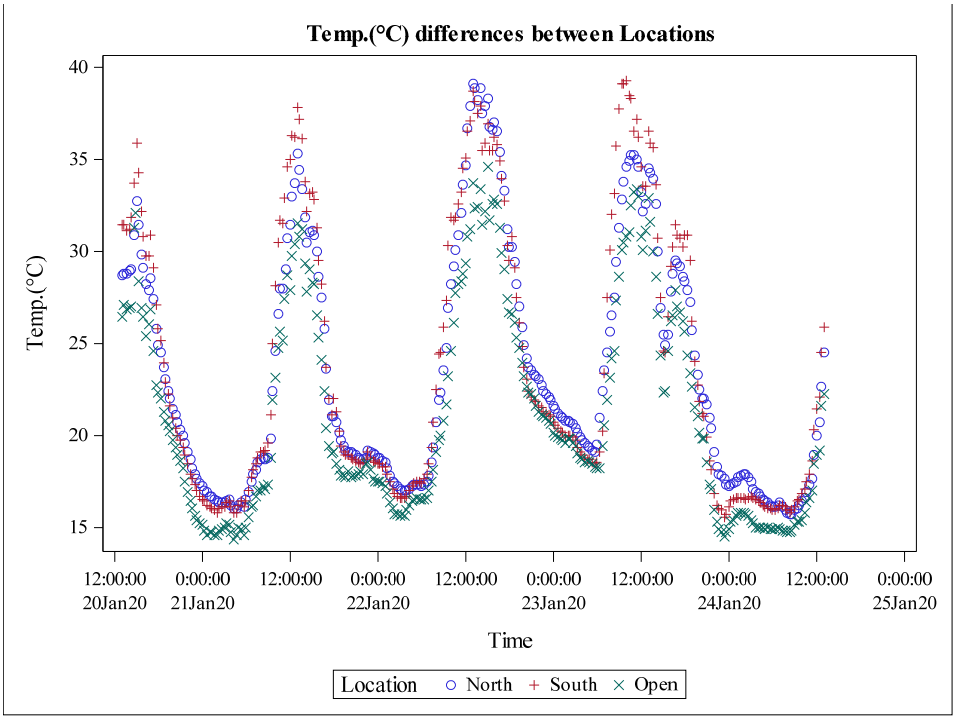

Figure 5: Temperature variations between the three locations - Summer period.

The analysis of field data revealed that the greenhouse slightly modulates the thermal conditions. The most distinct thermal differences occur during the winter period, with the summer thermal differences less differentiated. The thermal differences are also negligible at lower temperatures, but are most distinct during the peak insolation periods. This revealed both a greenhouse structure that is highly affected by direct shortwave radiation, and unable to retain the thermal energy gained during the daytime.

5. Results

Based on the data collected from the fieldwork, a simulation model was developed to replicate and verify the New Doornfontein case study. The model parameters established during the verification stage were in turn used to construct a theoretical model located in Tshwane.

5.1. Temperature impacts – Current weather conditions

The Tshwane simulation models were analysed using an indoor ambient temperature (T_a) comparison between the retrofitted and non-retrofitted models for the highly-insulated and poorly-insulated buildings over a seven-day period, during the summer and winter solstice and equinox periods. A correlation analysis of the indoor temperatures of the two models in the highly-insulated building revealed highly correlated conditions, ranging between 0.85 – 0.90 (Pearson's R) during the four test periods. In addition to closely correlated temperatures between the two building simulations, the analysis revealed that the retrofitted RTG led to a lower mean indoor temperature (- 0.73°C) on the top floor. The largest thermal impact was documented during the winter solstice period (June), with a 1.63°C lower mean temperature in the retrofitted simulation (Table 4). A full year analysis reveals that the retrofitting leads to the highest hourly temperature increase being in January (+ 3.19°C), while the largest hourly thermal loss is noted in June (-4.22°C).

Table 4: Comparison of the thermal difference once retrofitting a highly insulated building with RTGs

Measurement period	Mean temp diff (°C)	Max Temp (°C)	Min Temp(°C)	Diurnal swing base case vs retrofitted (°C); (% increase)
December 20-27	(-) 0.27	+ 0.39	(-) 1.94	3.01 vs 3.56 (18%)
March 20-27	(-) 0.42	(-) 0.18	(-) 1.72	3.92 vs 4.47 (14%)
June 20-27	(-) 1.63	(-) 1.15	(-) 3.02	3.86 vs 4.14 (7%)
September 20-27	(+) 0.01	+ 0.64	(-) 0.74	3.89 vs 4.41 (13%)

Importantly, the addition of the RTGs did not increase the indoor thermal stability, resulting in the mean diurnal swing increasing between 7-18% (Table 4). The largest single-day diurnal swing was documented in January, with a 87% increase (2.08 vs 1.11°C).

The retrofitting leads to a lower indoor temperature, which is most accentuated during the winter periods. This can be attributed to the additional shading that the RTGs provide and changes in the building envelope's albedo factor. While the largest thermal loss was documented during the winter period, during the hottest month in January periods of higher indoor thermal conditions were documented. While the higher roof insulation contributes to the beneficial impact of the RTG retrofitting, in the less insulated building simulation the role of thermal insulation was highlighted.

The lower insulated building simulation revealed contrasting results. While the correlational analysis documented a high correlation between the thermal performance of the retrofitted and non-retrofitted models, with a correlation of 0.95 to 0.97 (Pearson's R),higher mean ambient temperatures were consistently documented, ranging between +0.37°C (June) to +0.62°C (September) (Table 5). Unlike the highly insulated building simulation, retrofitting the poorly insulated building resulted in a constant indoor temperature increase with the highest thermal gain documented during the hottest period, +1.72°C in January. This can be attributed to the lower thermal insulation used in the building roof, resulting in the residual heat within the RTGs being conducted into the building interior. Interestingly, the thermal diurnal swing of the retrofitted building was less pronounced, with an average diurnal swing increase of between 1.2-3.6% (Table 5). In terms of the maximum daily diurnal swing, variations of a 5% improvement in June and 6% increase in March were documented.

Table 5: Comparison of the thermal difference once retrofitting a poorly insulated building with RTGs

Measurement period	**Ave temp diff (°C)**	**Max Temp (°C)**	**Min Temp(°C)**	**Diurnal swing base case vs retrofitted (°C); (% increase)**
December 20-27	+ 0.6	+0.78	+ 0.23	7.04 vs 7.12; (1.2%)
March 20-27	+ 0.52	+0.67	(-) 0.12	7.57 vs 7.85; (3.6%)
June 20-27	+ 0.37	+ 0.5	(-) 0.06	7.86 vs 7.98; (1.6%)
September 20-27	+ 0.62	+ 0.71	+ 0.37	9.60 vs 9.76; (1.7%)

5.2. Energy use impacts - Current weather conditions

To understand what the energy use implications of these indoor thermal differences would be on the top floors of the simulations, the analysis simulated energy consumption

differences if a comfortable indoor environment is retained. Using a typical centralised air-conditioner, the simulations considered changes in energy consumption, and heating and cooling loads stemming from the retrofitted RTGs.

Table 6: Analysis of the energy consumption increases resultant of the addition of an RTG to existing building.

	Highly insulated model			Poorly insulated model		
Period	**Non-Retrofitted (Total kWh)**	**Retrofitted (Total kWh)**	**Variation**	**Non-Retrofitted (Total kWh)**	**Retrofitted (Total kWh)**	**Variation**
Full Year	104.40kWh/m^2/pa. (297,569 kWh)	108.0kWh/m^2/p.a. (307,912 kWh)	+3.5%	99.29kWh/m^2/pa. (282,982 kWh)	102.39kWh/m^2/pa. (291,801 kWh)	+3.1%
Dec	(30,717 kWh)	(32,156 kWh)	+4.5%	(28,403 kWh)	(39,345 kWh)	+3.3%
Mar	(29,197 kWh)	(30,235 kWh)	+3.5%	(24,920 kWh)	(25.662 kWh)	+2.9%
Jun	(18,809 kWh)	(19,057 kWh)	+1.3%	(23,514 kWh)	(24,101 kWh)	+2.5%
Sept	(24,967kWh)	(25,795 kWh)	+3.3%	(21,489kWh)	(22,198 kWh)	+2.2%

In contrast to the thermal analysis, the overall building energy consumption analysis noted a minimal but constant increase throughout the various analysis periods in both the highly and poorly insulated models (Table 6). Retrofitting the highly insulated building revealed an energy consumption increase of 3.5% (104.40 vs 108.0 kWh/m^2/pa.), notably performing worse than the poorly insulated model. In both the highly and poorly insulated simulation models the highest energy consumption increases were documented during the hot summer period, September to March. The highest energy consumption increase, 4.5%, was documented in the highly insulated building simulation in December. Conversely, the smallest consumption increases occurred in the winter period (June), with a negligible increase in the highly insulated model (+1.3%), but a 2.5% increase in the poorly insulated model.

Although the overall energy consumption increase is small, the adverse effects of the retrofitted RTGs were more pronounced in terms of the impacts in the heating and cooling loads on the top floor. In both the highly and poorly insulated models these loads increased with 9.9% and 10.2%, respectively. The largest increase was documented in the poorly insulated building where the cooling load increased with 17.6% (22,459 vs 26,408 kWh). Although this same poorly insulated model revealed a 2.8% decrease in heating loads, this was not evident in the highly insulated model where the heating load increased from 0.0kWh to 36kWh once retrofitted. This revealed a negligible loss in shortwave radiation energy due to the shading effect of the RTGs in winter.

The dramatic change in the performance of the highly insulated building simulation highlighted the drawback when unmanaged residual heat is collected in temperate to hot

climatic conditions. When a strategy to ameliorate the indoor temperatures is employed, in this case air-conditioning with a cooling set point of 25°C, the cooler indoor temperatures shift the energy balance. This results in the retrofitting strategy adversely affecting the building performance. As noted in Fourier's law on thermal conductance through isotropic bodies, the higher thermal difference between the spaces shifts the performance balance in the highly insulated building. As a result, any benefits due to changes in albedo factors and additional shading are lost.

Furthermore, the simulations also revealed the complexity around the use of insulation material in these temperate to hot climates. While additional roof insulation improved the indoor thermal conditions, the improved insulation also adversely affected the building performance in dispelling excess thermal energy within the building interior due to internal thermal gains, and harnessing any beneficial impacts of the residual heat contained in the RTG during cooler periods. This highlighted the importance of holistically adjusting and optimising both the building performance specifications and the RTGs' bioclimatic design.

5.3. Simulations of 2100 climate change affected conditions

These same models were simulated under expected climate conditions that replicate A2 climate change scenarios by the year 2100 (IPCC, 2000). Under the higher thermal conditions (A2 scenario) the retrofitting strategy of the higher insulated model shifted from a beneficial solution to a negative state. As a result, the retrofitting strategy led to higher indoor temperatures ($T_{a\ mean}$=+0.48°C), with the highest thermal difference recorded in the summer season. The maximum hourly thermal increases ranged between +3.03 to +4.53°C. On the other hand, the results from the lower thermally insulated model were near identical to the current climatic conditions, with $T_{a\ mean}$ increases of between +0.49 to +0.73°C. The thermal comparisons revealed that, unlike the poorly insulated model, the highly insulated model is more affected by the retrofitting strategy under warmer conditions.

Simulating the energy consumption of retrofitted buildings under A2 conditions further supported the findings from the thermal comparisons. While the highly insulated model performed better than the poorly insulated building in absolute terms (127.05 vs 131.70 kWh/m^2/p.a.), the impact of the retrofitted RTGs was more substantial in the highly insulated building with the annual energy consumption increasing from 3.5% to 3.9% in the A2 scenarios (Tables 6 & 7). This translated to an 11% higher adverse impact. The simulation concluded that the highest energy consumption increases occurred during the hottest period, in this case a 5.7% increase in December. Similarly, the largest cooling load increase (+13.4%) was noted on the top floor of the highly insulated model.

Table 7: Comparison of the energy consumption variations under 2100 conditions.

	Whole building			Top floor only		
	Energy use intensity (kWh/m^2/pa)	Energy use Dec (kWh)	Energy use Jun (kWh)	Cooling load (kWh)	Heating Load (kWh)	Total (kWh)
Highly insulated model	122.26	35,076	21,246	54,522	0.0	54,522
Retrofitted highly insulated model	127.05	37,105	21,415	61,850	0.0	61,850
Variation (%)	+ 4.78 (+3.9%)	+ 2,029 (+ 5.7%)	+ 169 (+ 0.7%)	+ 7,328 (+ 13.4%)	0.0 (0%)	+ 7,328 (+ 13.4%)
Poorly insulated model	127.67	40,021	20,054	58,704	3,260	61,963
Retrofitted poorly insulated model	131.70	41,253	20,610	65,659	3,046	68,705
Variation (%)	+ 4.03 (+ 3.2%)	+ 1,232 (+ 3.0%)	+556(+ 2.8%)	+ 6,955 (+11.8%)	(-) 214 (- 6,6%)	+ 6,742 (+10,8%)

The 2100 climate change induced simulations revealed that the retrofitting strategy provides limited thermal control in the long term under hotter climate conditions. Furthermore, while less adverse impacts were experienced when retrofitting a poorly insulated building, negative impacts were documented throughout all the simulations.

6. Discussion

While several studies promote thermal and other co-benefits from the integration of RTGs with the built environment (Benis et al., 2017; Nadal et al., 2018; Sanye-Mengual et al., 2018), these cannot be taken for granted. As seen in this study, the choice of construction material, contextual conditions, and the lack of design solutions to harness residual energy, can result in adverse thermal effects. The study supports findings by Benis et al. (2015) which analysed the thermal impact of RTGs in the Mediterranean context, arguing that merely positioning RTGs on roofs can exacerbate the high indoor thermal conditions during the hot summer seasons.

As this study considers the application of RTGs in hot and dry conditions (Koppen-Geiger: CwA), the additional residual thermal energy proves to be problematic in climates where cooling is critical. This misalignment of thermal energy is further intensified by the building function, as the study reveals that office buildings in hot, subtropical conditions require cooling even in the winter season. As a result, the unmanaged thermal energy does not improve the indoor conditions, and the systemic integration of resources and infrastructure between the buildings and RTGs structures is required to achieve any thermal co-benefits.

Finally, the building properties themselves cause adverse impacts, as the poorly-insulated building simulation revealed that the lower roof insulation performed poorly under higher thermal conditions in absolute terms.

The poor performance of the RTGs highlights the concern of promoting untested assumptions in the urban agriculture discourse, risking inexpedient policy development and ineffective funding allocation (Goldstein et al., 2016). Transferring and applying technologies from diverse contexts and climatic conditions must therefore be carefully considered. In this case, the analysis of passively controlled non-integrated RTGs in the Southern African context highlighted the importance of testing technologies before promoting them as context-specific solutions.

It may be possible to mitigate the negative energy and thermal impacts by improved integration of RTG farming with the host building, following a more systemic approach to managing thermal energy, and using different material and technology choices.

Controlling and storing the thermal energy to use when needed in the host building or in the farm itself can stabilise the energy consumption and improve the indoor environment. For example, a study by Sanye-Mengual et al. (2018) suggested that surplus thermal energy available in hot climates can be used to stimulate higher plant yields. Care must be taken though, as the crop-canopy temperatures in greenhouses are often already in the upper regions of the optimal growing conditions, as noted by South African urban farmers and Thipe et al. (2017). Furthermore, the expected climate change impacts will certainly increase this beyond the optimal growing range (DEA, 2013). As result, the utility potential of the added thermal energy must be carefully considered.

While the design of alternative RTG resolutions were delimited from the study, the findings highlighted important factors to consider or test. In contrast to the existing RTGs that only focus on cost saving and as a result use a composite envelope of poly-EVA and knitted HDPE shade netting, the high solar exposure of these greenhouses can be harnessed. By lining them with thin-film photovoltaic cells with high transparency, these greenhouses can function as small-scale energy-generating plants whilst addressing the issues of overexposure. The greenhouse structures and forms are also typical of a single one-size-fits-all solution. Adjusting these to increase or decrease solar exposure with operable vents to actively manage the indoor thermal energy can potentially improve the performance of the RTGs. Finally, improving the insulative capacity of the RTGs' envelopes, and collecting and storing the thermal energy through heat exchangers can translate into co-benefits to the associated building and improve the indoor environment of the RTGs.

Adjusting the building along with the RTG design to maximise the co-benefits of this retrofitting strategy is vital though. It is further important to note that increasing the adaptive capacity of the RTGs will be critical, as continued flexibility in the design and optimisation of the built form, technology and the crop choice will be needed to leverage current and future co-benefits in changing climate scenarios.

7. Conclusion

This study explored the co-benefits that the integration of agriculture with the built environment enables, and specifically focused on the thermal impact of retrofitting passively controlled, non-integrated RTGs on existing buildings in hot temperate Southern African climates (CwA & CwB) in current and predicted future climate conditions.

The simulations revealed that the use of RTGs on both highly insulated and poorly insulated buildings can have adverse thermal and energy effects. While the simulations documented an average temperature decrease of 0.73°C in the highly insulated models, the use of the RTGs unexpectedly led to a 3.5% increase in overall energy consumption when the buildings use artificial heating or cooling. Furthermore, the simulations of the same highly insulated model under future climate change induced conditions reveal that the RTGs increased the adverse impact on annual energy consumption by 11%.

The findings, therefore, highlight the importance of designing locally appropriate technologies and not simply transferring successful technologies from alternative contexts without the necessary adjustments. By providing more empirical data on the thermal performance and associated impacts of RTGs currently implemented in Southern African cities, this study can inform the adjustments needed to improve the performance of this land-use form.

As further research, this study proposes using the model information and findings to develop RTG solutions that are appropriate to hot temperate climates, and take cognisance of the expected hotter climate change induced conditions. The simulations can consider the design resolution of these RTGs under current and future climatic conditions. The systemic integration of these RTGs with the built environment can ultimately improve their resource efficiency, as achieved in the ICTA-ICP building in Barcelona (Nadal et al. 2017), and the functional integration with the built environment can provide other co-benefits as proposed by Sanyé-Mengual et al. (2018).

8. Acknowledgements

The authors wish to thank the rooftop farmers that made their farms available for data collection, WIBC that facilitated the process, and the reviewers that provided comments to

improve the article. The financial assistance (Grant no. 78649) of the South African National Research Foundation (NRF)toward the research is hereby acknowledged.

9. References

Al-Helal, I.M., Abdel-Ghany, A.M., 2011. Measuring and evaluating solar radiative properties of plastic shading nets. Solar Energy Materials & Solar Cells 95, 677-683.

Allen, R.G., Pereira, L.S., Raes, D., Smith, M., 1998. Crop evapotranspiration - Guidelines for computing crop water requirements - FAO Irrigation and drainage, Irri. Drain Paper 56. Rome.

ASHRAE, 2017. ASHRAE Handbook - Fundamentals. ASHRAE, Atlanta.

Benis, K., Gomes, R., Vicente, R., Ferrão, P., Fernández, J.E., 2015. Rooftop Greenhouses: LCA and Energy Simulation, in: CISBAT 2015. Lausanne, pp. 95–100.

Benis, K., Reinhart, C., Ferr, P., 2017. Development of a simulation-based decision support work flow for the implementation of Building-Integrated Agriculture (BIA) in urban contexts. J. Clean. Prod. 147, 589–602. https://doi.org/10.1016/j.jclepro.2017.01.130

Berge, B., 2009. The Ecology of Building Materials, 2nd Edition. Architectural Press, Oxford.

Beveren, P.J.M. Van, Bontsema, J., Straten, G. Van, Henten, E.J. Van, 2015. Minimal heating and cooling in a modern rose greenhouse. Appl. Energy 137, 97–109. https://doi.org/10.1016/j.apenergy.2014.09.083

Caplow, T., 2009. Building integrated agriculture: Philosophy and Practice, in: Heinrich Böll Foundation (Ed.), Urban Futures 2030. Urban Development and Urban Lifestyles of the Future. Heinrich Böll Foundation, Berlin, pp. 54–58.

Castleton, H.F., Stovin, V., Beck, S.B.M., Davison, J.B., 2010. Green roofs; Building energy savings and the potential for retrofit. Energy Build. 42, 1582–1591. https://doi.org/10.1016/j.enbuild.2010.05.004

Cohen, J.A., 1988. Statistical power Analysis for the Behavioural Sciences, Second Edition.. Lawrence Erlbaum Associates, New Jersey.

Conradie, D.C.U., 2017. Calculating solar protection for buildings in South Africa. Green Building Handbook, 11, 48-59.

Davie, L., 2018. Farms in the sky over Joburg. http://www.jicp.org.za/urban-agriculture-initiative/ (accessed 03.20.19).

DEA, 2013. Long-term Adaptation Scenarious Flagship research programme (LTAS) for

South Africa. Climate Trends and Scenarious for South Africa. Pretoria.

DOE, 2019. Market Assessment of Residential and Small Commercial Air Conditiones in South Africa. Pretoria.

Dubbeling, M., Zeeuw, H. De, 2011. Urban Agriculture and Climate Change Adaptation: Ensuring Food Security Through Adaptation, in: Otto Zimmerman, K. (Ed.), Resilient Cities: Cities and Adaptation to Climate Change -Proceedings of the Global Forum 2010. Springer, Dordrecht, pp. 441–449.

Engineering Toolbox, 2019. The Heat specific Capacity of Materials. https://www.engineeringtoolbox.com/specific-heat-capacity-d_391.html (accessed on 08.24.19).

ENVIMET, 2018. ENVIMET Homepage. https://www.envi-met.com/intro/ (accessed 11.16.18).

Goldstein, B., Hauschild, M., Fernandez, J., Birkved, M., 2016. Urban versus conventional agriculture , taxonomy of resource profiles : a review. Agron. Sustain. Dev. 36, 1–19. https://doi.org/10.1007/s13593-015-0348-4

Graamans, L., Baeza, E., Dobbelsteen, A. Van Den, Tsafaras, I., Stanghellini, C., 2018. Plant factories versus greenhouses: Comparison of resource use efficiency. Agric. Syst. 160, 31–43. https://doi.org/10.1016/j.agsy.2017.11.003

IES, 2018. Software Validation and Approval. https://www.iesve.com/software/software-validation (accessed on 02.05.2020).

IPCC, 2000. Emmisions Scenarios. Cambridge, UK.

Liang, T.C., Hien, W.N., Jusuf, S.K., 2014. Effects of vertical greenery on mean radiant temperature in the tropical urban environment. Landsc. Urban Plan. 127, 52–64. https://doi.org/10.1016/j.landurbplan.2014.04.005

Monteith, J.L., 1965. Evaporation and Environmnet. Symp. Soc. Exp. Biol. 19, 205–234.

Nadal, A., Llorach-massana, P., Cuerva, E., López-capel, E., Ignacio, J., Josa, A., Rieradevall, J., Royapoor, M., 2017. Building-integrated rooftop greenhouses: An energy and environmental assessment in the mediterranean context. Appl. Energy 187, 338–351. https://doi.org/10.1016/j.apenergy.2016.11.051

Nadal, A., Pons, O., Cuerva, E., Rieradevall, J., Josa, A., 2018. Rooftop greenhouses in educational centers: A sustainability assessment of urban agriculture in compact cities. Sci. Total Environ. 626, 1319–1331. https://doi.org/10.1016/j.scitotenv.2018.01.191

Nasr, J., Komisar, J., Zeeuw, H. De, 2017. A Panorama of Rooftop Agriculture Types, in: Orisini, F. (Ed.), Rooftop Urban Agriculture. Springer International, pp. 9–29. https://doi.org/https://doi.org/10.1007/978-3-319-57720-3_21

Nelli, L.C., 2020. Urban Regeneration with Rooftop Farming Pilot Projects, in: Sayigh, A. (Ed.), Green Buildings and Renewable Energy. Springer Nature, pp. 501–511. https://doi.org/https://doi.org/10.1007/978-3-030-30841-4_36

Nijskens, J., Deltour, J., Coutisse, S., Nisen, A., 1984. Heat transer through covering materials of greenhouses. Agric. For. Meteorol. 33, 193–214.

Orsini, F., 2020. Innovation and sustainability in urban agriculture : the path forward. J. Consum. Prot. Food Saf. 10–11. https://doi.org/10.1007/s00003-020-01293-y

Orsini, F., Dubbeling, M., Gianquinto, G., 2015. Multifunctional rooftop horticulture: a promising strategy for intensifying horticulture production in cities. Chron. Horticult. 4, 12–17.

Sanyé-mengual, E., Cerón-palma, I., Oliver-solà, J., Ignacio, J., Rieradevall, J., 2015. Integrating Horticulture into Cities : A Guide for Assessing the Implementation Potential of Rooftop Greenhouses (RTGs). Urban Technol. 0, 1–25. https://doi.org/10.1080/10630732.2014.942095

Sanye-Mengual, E., Martinez-blanco, J., Finkbeiner, M., Cerda, M., Camargo, M., Ometto, A.R., Velasquez, L.S., Villada, G, Niza, S., Pina, A., Ferreira, G., ., Oliver-Solá, J., Montero, J.I., Rieradevall, J., 2018. Urban horticulture in retail parks: Environmental assessment of the potential implementation of rooftop greenhouses in European and South American cities. J. Clean. Prod. 172, 3081–3091. https://doi.org/10.1016/j.jclepro.2017.11.103

Serir, L., Bournet, P.E., Benmoussa, H., Mesmoudi, K., Physics, E., 2012. Thermal Simulation of a Greenhouse under a Semi-Arid Climate. Acta Hortic. Hortic. 927, 635–642.

Skelhorn, C.P., Levermore, G., Lindley, S.J., 2016. Impacts on cooling energy consumption due to the UHI and vegetation changes in Manchester, UK. Energy Build. 122, 150–159. https://doi.org/10.1016/j.enbuild.2016.01.035

South Africa, 2011. SANS 10400XA: Energy usage in Buildings. Government Printer, Pretoria, South Africa.

Specht, K., Siebert, R., Hartmann, I., Freisinger, U.B., Sawicka, M., Werner, A., Thomaier,

S., Henckel, D., Walk, H., Dierich, A., 2014. Urban agriculture of the future : an overview of sustainability aspects of food production in and on buildings 33–51. https://doi.org/10.1007/s10460-013-9448-4

StepSA, 2020. Climate indicators Koppen-Geiger climate classifications. http://stepsa.org/climate_koppen_geiger.html (accessed 11.18.2020).

Thipe, E.L., Workneh, T., Odindo, A., Laing, M., 2017. Greenhouse Technology for Agriculture Under Arid Conditions. Sustain. Agric. Rev. 22, 37–55. https://doi.org/10.1007/978-3-319-48006-0

Thomaier, S., Specht, K., Henckel, D., Dierich, A., Siebert, R., Freisinger, U.B., Sawicka, M., 2014. Farming in and on urban buildings : Present practice and specific novelties of Zero-Acreage Farming (ZFarming). Renewable Agriculture and Food Systems 30(1), 43-54. https://doi.org/10.1017/S1742170514000143

Table 8: Appendix - list of symbols and abbreviations used.

Symbol	Description	Unit
R-value	Thermal resistance	m^2KW^{-1}
U-value	Thermal conductivity/transmissivity	$Wm^{-2}K^{-1}$
T_{tot}	Total envelope transmissivity	$Wm^{-2}K^{-1}$
SHGF	Solar heat gain factor	
°C	Degrees Celsius	
T_a	Ambient temperature	°C
T_g	Globe Temperature	°C
RH	Relative humidity	%
Qrad	Energy gains to insolation	J
Qinf	Energy losses to infiltration and leakage	J
Qconv	Energy losses to convection	J
Qcond	Energy gains or losses to conduction	J
Qlat	Latent thermal energy conversion	J
Qevap	Energy losses to evapotranspiration	$W.m^{-2}$
I_{rad}	Total incident radiation	$MJ.m^{-2}$
G	Heatflux	$MJ.m^{-2}day^{-1}$
e_s	Saturated vapour pressure	kPA
e_a	Actual vapour pressure	kPA
y	Psychrometric constant	kPA
u_2	Wind speed	$m.s^{-1}$
Δ	Vapour pressure curve	$kPA°C^{-1}$